

# Fiber Laser Coherent LIDAR for Wake-Vortex Hazard Detection

Mehmetcan Akbulut, Shantanu Gupta, Horacio Verdun  
 Fibertek, Inc.  
 13605 Dulles Technology Dr.  
 Herndon, VA 20171 USA  
[makbulut@fibertek.com](mailto:makbulut@fibertek.com)

## 1. Introduction

Active remote sensors are turning into indispensable tools for aviation. Especially, coherent lidar systems which can detect atmospheric aviation hazards such as wake-vortices, air drafts, wind shear and turbulence have received wide interest. Such lidars have been deployed with increasing numbers at airports and research facilities around the world. Some of the common aviation safety applications include landing and takeoff in adverse conditions and aircraft spacing optimization at airports.

The most widespread implementation of a coherent lidar transmitter is a high energy (milliJoules) and low repetition rate (multi Hz) solid-state laser<sup>1-5</sup>. The higher energy is desirable to reach further range and relax requirements on the receiver. However, the low repetition rate is not attractive due to possible fluctuations of the laser and the atmospheric conditions from pulse to pulse, yielding inaccurate measurements. Additionally, the lower repetition rate reduces the overall measurement time for a lidar scan. In contrast, a higher repetition rate enables faster time-resolved measurements, and provides capability for averaging the measurements to smooth out speckle and other distortions. The solid-state laser technology cannot provide repetition rates higher than ~few kHz due to thermal problems, whereas fiber-optic based coherent lidars can provide up to GHz repetition rates, but with lower energy levels<sup>6-8</sup>. Additional benefits of fiber-optic technology arises from the size weight and power (SWaP) improvements, flexible installability of subsystems, robustness and maturity of component technology, availability of ultra-stable local oscillator lasers, and powerful pulse formatting capabilities for multi-function lidar operation. These characteristics make fiber-optic lidars ideal tools for airborne applications, where the “electrical power

consumption” and “physical volume per functionality” is critical.

In this paper, we describe such a fiber-optic coherent lidar system that is designed for airborne wake-vortex hazard detection. In the next section we discuss the challenges for airborne wake-vortex detection. The following section shows system level details, performance simulations, and the achievements to date on the lidar development. Finally, we present some preliminary application-based experimental results of the lidar system in the laboratory.

## 2. Airborne lidar wake-vortex detection

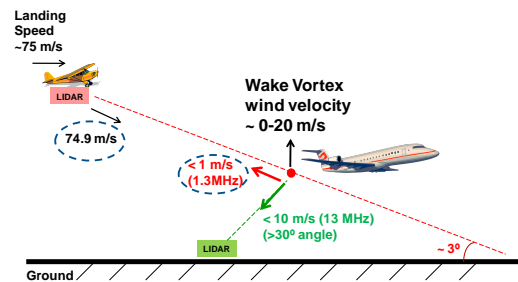


Figure 1 – Wake-vortex lidar sensor operation

A cartoon depicting the operation of a wake-vortex lidar sensor during aircraft landing is shown in Figure 1. The figure depicts both an airborne, and a ground-based lidar system. The most obvious advantage of the ground-based lidar is the non-limitations on SWaP. However, there are bigger technical advantages of ground-based sensing as shown in the cartoon, such as having access to a much larger cross-section of the wake-vortex wind vector, and not worrying about platform motion correction (since Doppler sensing measures relative velocity). In this scenario, the airborne lidar requires very high wind velocity resolution (~0.1 m/s), and highly accurate platform-motion information to yield valid axial lidar data. These specifications put rigid limits on the lidar design as discussed in the next section.

### 3. Fiber Optic Coherent Lidar

#### Lidar System

The overall lidar system diagram is shown in Figure 2. The lidar consists of three main subsystems: a main unit that houses the lidar transmitter, receiver and control electronics; an optical head that is remotely installed and containing the transmit/receive switch, telescope, and scanner; and computer hardware for user interface, data display, and storage.

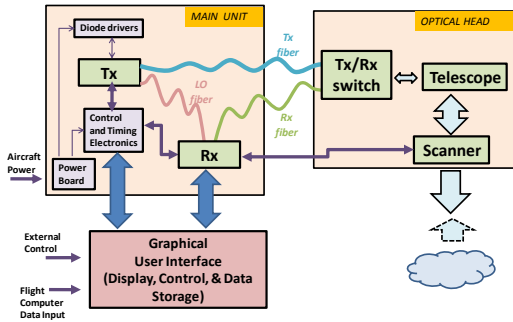


Figure 2 – Overall lidar system diagram

The performance of the lidar system in terms of range, velocity resolution, and accuracy can be degraded by various noise sources. For example, the range can be reduced at high altitudes by the low density of atmospheric particles, and the resolution can be reduced by localized gradients in wind patterns that increase the Doppler linewidth. In this system design, we focused on the parameters that we can control. For instance, based on certain scanning geometries, and the fiber-optic system capabilities, we chose the repetition rate of the lidar transmitter to be 25 kHz. Additionally, for a good compromise between spatial resolution and velocity resolution, we chose the pulse width as ~800 ns. This yields a ~1.5 MHz Doppler linewidth, which is enough to track 0.1 m/s wind velocity changes (~0.13 MHz at 1.55 μm wavelength). The master/local oscillator amplitude and phase noise is also important for best signal-to-noise ratio (SNR). Therefore, we chose ultra-low noise laser sources with ~kHz level linewidth, and -140 dBc/Hz amplitude noise. This also ensures long term stability and repeatability of lidar measurements. In terms of receiver design, we opted to use a balanced coherent detection scheme with low noise analog electronic amplifiers, and on-board Gigabit rate real-time sampling and signal processing for best receiver performance.

#### Lidar Performance Simulations

In order to assess the lidar performance, and gain insight on certain scanning geometries, we conducted simulations based on TASS data. These simulations utilized detailed models developed by Fibertek, and included many atmospheric and optical parameters. A sample simulation result is shown in Figure 3. The left column shows the TASS data for various wake ages, and the left column shows what the designed lidar system would measure. The wake-vortex and the evolution that the lidar simulation gives matches well with the TASS data even at degraded spatial resolution.

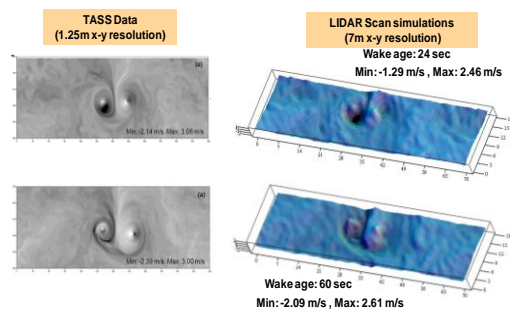


Figure 3 – Overall lidar system diagram

Figure 4 shows the simulations of range vs. lidar pulse energy. This simulation assumes a SNR of 6, and receiver aperture of 5 cm. With 25 kHz repetition rate, 40 averages are enough to yield greater than 1.5 km range at 100 μJ pulse energy. Even in this scenario with averaging, a point-measurement update rate of >600Hz can be achieved. With more averages, greater lidar range can be achieved at the expense of measurement update rate.

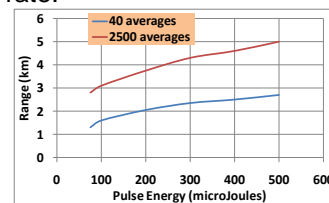


Figure 4 – Lidar range vs. pulse energy simulation

#### Lidar Transmitter Development

The lidar system was chosen to operate at 1.55 μm wavelength due to the availability of mature component technologies at this band, and the eye-safety concerns. The transmitter is based on a fiber-optic master oscillator-power amplifier (MOPA) architecture (Figure 5). The master oscillator is a ultra-low noise semiconductor distributed feedback (DFB) laser. It has ~2.5 kHz linewidth, and relative intensity

noise (RIN) of -140 dBc/Hz (at 20 kHz) as measured by Fibertek (Figure 6).

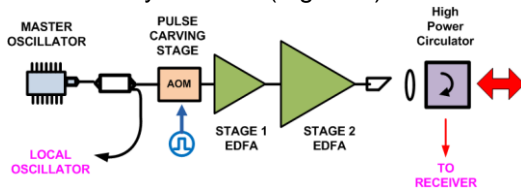


Figure 5 – Lidar transmitter architecture

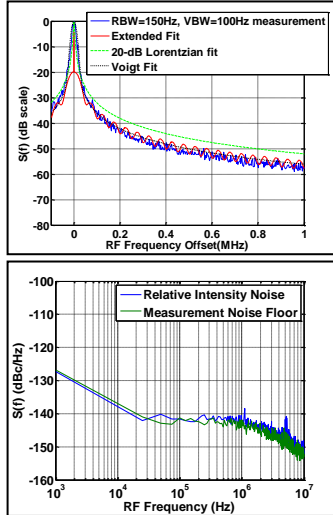


Figure 6 – Master oscillator linewidth (top) and RIN (bottom) measurements

The master oscillator is operated in continuous-wave mode for the lowest noise and highest stability. An acousto-optic modulator (AOM) is used to carve the 800ns pulses at 25 kHz. The AOM serves dual purpose: one as the high-extinction ratio pulse generator, and second as the frequency shifter for Doppler detection. The AOM frequency was set at ~55 MHz.

For the fiber amplifier chain, commercially available polarization-maintaining (PM) erbium-doped gain fiber was utilized. At each amplification stage, fibers gain increasing mode field diameter (MFD) was used to minimize nonlinear effects. The largest nonlinear effect for our system was identified as the Stimulated Brillouin Scattering (SBS). Calculations and experiments showed that SBS limited the energy that can be obtained from the final amplifier stage to ~120  $\mu$ J at 25 kHz (3 Watts) with the 800 ns pulse width. By utilizing proprietary SBS mitigation techniques, we were able to achieve up to ~560  $\mu$ J at 25 kHz (~14W), which was limited by the available pump power. Figure 7 shows the output power vs. coupled pump power along with estimated efficiency of the fiber amplifier. We estimated up to ~21% optical-to-optical efficiency at the highest energy level. Based on the lidar

Figure-of-Merit (FOM) description<sup>1</sup> of “Energy\*sqrt(Repetition rate)”, this lidar system yields FOM of ~19 mJ. $\sqrt$ Hz for 120  $\mu$ J energy, and ~88 mJ. $\sqrt$ Hz for 560  $\mu$ J output energy.

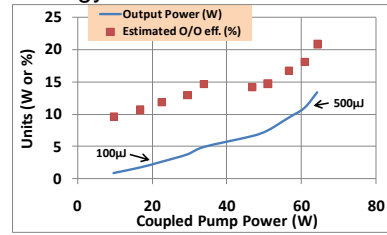


Figure 7 – Fiber amplifier output power and optical/optical efficiency vs. coupled pump power

The polarization extinction ratio was measured as ~17 dB, and the  $M^2$  was estimated to be less than 1.2 based on beam profile measurements (Figure 8). The minimal distortions in the beam profile is due to aberrations from the lens that was used to focus the beam on the camera. Figure 9 shows the forward (top) and backward (middle) optical spectrum at 560  $\mu$ J energy demonstrating minimal amplified spontaneous emission (ASE) and SBS. The spectrum plots show relative measurements, as the total absolute backreflected energy was measured as ~0.1  $\mu$ J. Figure 9 bottom shows the photodetected optical pulses, which show mild pulse steepening.

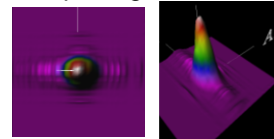


Figure 8 – Beam profile measurement

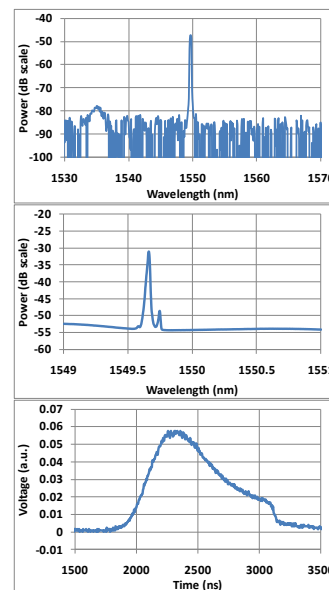


Figure 9 – Forward optical spectrum (top), backward optical spectrum (middle), and time-domain (bottom) at 560  $\mu$ J energy

### Lidar Receiver Development

We have designed the lidar receiver to operate as a balanced coherent detection system with a high gain, low noise analog front-end. Based on our calculations and earlier Fibertek-built receivers, we expect to have a receiver sensitivity of  $\sim 0.03$  pW (SNR=6). At the back-end, we digitize and signal-process the data at GHz rates for fast data display and storage capability.

The receiver is designed to have a  $\pm 20$  m/s velocity range with a  $\sim 0.1$  m/s resolution. The spatial resolution will be  $\sim 40$ -120 meters determined by the time-gate slices. Additionally, the receiver will acquire platform motion information from an external INS-GPS unit, and correct for platform velocity (20 – 200 m/s). This enables the lidar to be operational in various aircraft altitudes and scanning angles.

#### 4. Preliminary lidar data

As a means of preliminary testing, we have conducted experiments in the laboratory with the lidar transmitter and a partially-completed lidar receiver (in that there are only a few electronic amplifier stages). First, we attenuated the lidar transmitter output to  $\sim \mu$ W power levels, and coupled it through 25 km single mode fiber. This is equivalent to a  $\sim 18.5$  km lidar range in air, plus much stronger depolarization effects. The resulting receiver output is shown in Figure 10. The Doppler linewidth is on the order of  $\sim 1.5$  MHz, the peak is at 55 MHz (AOM frequency) and highly coherent sinc-function like structure is observed as expected. In a second experiment, we directed the full transmitter output at an angle to a rotating motor with a variable angular velocity (controlled by the motor voltage). The diffuse reflection from the motor was collected with a lens into the receiver single mode fiber. The measured power coupled into the fiber was  $\sim 100$  pW (4 fJ energy). Figure 11 shows the Fourier-transform of the digitized time-domain data at various motor voltage levels (thus angular velocities). Even with this partially-completed receiver, we were able to demonstrate SNR greater than 10 and a peak-measurement resolution of  $\sim 0.1$  MHz.

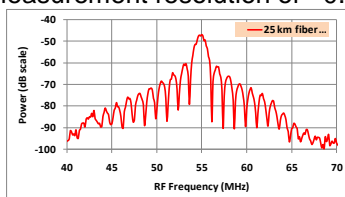


Figure 10 – Lidar testing with 25km fiber delay

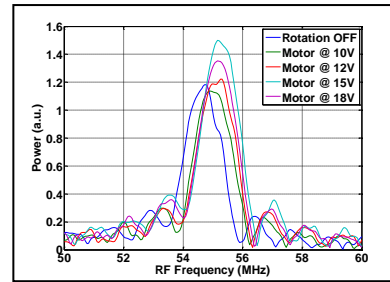


Figure 11 – Fourier-transform of digitized data for various voltages applied to the rotating motor

#### 5. Conclusion

We have demonstrated a  $1.55 \mu\text{m}$  fiber-optic coherent lidar system with greater than  $500 \mu\text{J}$  energy at 25 kHz and  $\sim 1.5$  MHz Doppler linewidth. We believe this lidar has the potential for aviation applications such as airborne wake-vortex hazard detection.

#### 6. Acknowledgements

This work was funded by NASA Langley Research Center through SBIR program NNX10CB26C.

#### 7. References

1. S.M.Hannon, et.al., "Next Generation Doppler Lidar Sensor at  $1.6 \mu\text{m}$ ", Proc. 14<sup>th</sup> CLRC (2007).
2. U.Singh, et.al., "Compact, High Energy 2-micron Coherent Doppler Wind Lidar Development for NASA's Future 3-D Winds Measurement from Space", NASA Tech. Rep., (2010).
3. S.Rahm, et.al., "Characterization of Aircraft Wake Vortices by Airborne Coherent Doppler Lidar", Jour. Aircraft, vol.44, 799-805 (2007).
4. F.Kopp, et.al., "Characterization of Aircraft Wake Vortices by 2- $\mu\text{m}$  Pulsed Doppler Lidar", Jour. Atm. Ocean. Tech., vol.21, 194-206 (2003).
5. D.Douxchamps, et.al., "On-board axial detection of wake vortices using a 2- $\mu\text{m}$  LiDAR", IEEE Trans. Aero. Electron. Sys., vol.44, 1276-1290 (2008).
6. A.Dolfi-Bouteyre, et.al., "Pulsed 1.5- $\mu\text{m}$  LIDAR for Axial Aircraft Wake Vortex Detection Based on High-Brightness Large-Core Fiber Amplifier", IEEE JSTQE, vol.15, 441-450 (2009).
7. H.Inokuchi, et.al., "Development of an airborne wind measurement system", Proc. SPIE, vol.7382, 738205 (2009).
8. S.M. Spuler, et.al., "Optical fiber-based laser remote sensor for airborne measurement of wind velocity and turbulence", Appl. Opt., vol.50, 842-851 (2011).